

Study of a Reversible Gas Phase Reaction: An Integrated Physical Chemistry Project

João Pedro Malhado, Miguel Tavares, and Mário N. Berberan-Santos*

Centro de Química-Física Molecular, Instituto Superior Técnico, 1049-001 Lisboa, Portugal,
berberan@ist.utl.pt

Received July 25, 2003. Accepted October 16, 2003.

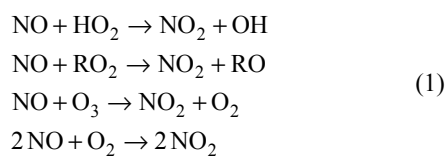
Abstract: The reversible gas phase reaction dinitrogen tetroxide to nitrogen dioxide is very suitable for an integrated physical chemistry project incorporating thermodynamics, statistical mechanics, spectroscopy, and kinetics. Furthermore, nitrogen oxides are molecules of current interest given their important role in atmospheric chemistry. Only relatively common equipment and chemicals are required for the experiment. It consists of the synthesis of NO₂ and of the study of the UV–vis electronic absorption spectrum of the NO₂/N₂O₄ gas mixture as a function of temperature. From the analysis of the spectra, the absorption spectra of the pure constituents are obtained as well as the temperature dependence of the equilibrium constant of the reaction. From this dependence, the enthalpy and the entropy of the reaction are obtained. The values are analyzed and compared with statistical mechanical calculations. The kinetics of the reaction is also discussed.

Introduction

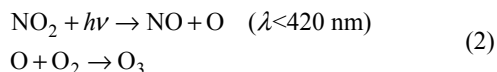
The nitrogen oxides are a family of compounds of industrial, biological, and environmental importance. Furthermore, some of their physicochemical properties are quite interesting. In Table 1, some properties of selected nitrogen oxides that are gases at room temperature are displayed [1].

Nitrogen dioxide, first characterized by Dulong [2], stands out as the only common nitrogen oxide that has a color. The fumes of concentrated nitric acid, for instance, are yellow-brown owing to NO₂. Part of the yellow-brown tint of polluted air in urban areas is also due to NO₂.

Nitrogen dioxide is present in the atmosphere in low but significant concentrations. Most of the tropospheric NO₂ originates in combustion reactions where some N₂ oxidation takes place. The primary oxidation product is NO, but this compound readily transforms quantitatively into NO₂ at atmospheric temperatures [3, 4]. The formation of NO₂ occurs mainly by the reactions [3, 4]



where RO₂ is an alkyl peroxide radical, for instance CH₃OO•. Nitrogen dioxide is the main source of tropospheric ozone, acting according to the photochemical reaction [3]



For this reason, NO₂ is of great importance in atmospheric chemistry, namely in the processes associated with photochemical smog [3]. It also plays a role in acid rain and in stratospheric ozone depletion [3].

The nitrogen dioxide molecule possesses an unpaired electron, essentially located in the nitrogen atom, and has for this reason some propensity to dimerize forming the colorless dinitrogen tetroxide,



The dimerization process occurs by an elementary reaction with negligible activation energy, as is typical of the recombination of simple radicals. The N–N dimer bond energy is, however, small (only 57 kJ mol⁻¹), and the dimer is unstable at room temperature. The reverse reaction, a unimolecular dissociation, is for this reason also an important process at room temperature



It is, therefore, the study of the reversible reaction



that is the subject of the present work. It consists of the synthesis of NO₂ and the study of the UV–vis electronic absorption spectrum of the NO₂/N₂O₄ gas mixture as a function of temperature. From the analysis of the spectra, the absorption spectra of the pure constituents are obtained as well as the temperature dependence of the equilibrium constant of the reaction. From this dependence, the enthalpy and the entropy of the reaction are obtained. The values are analyzed and compared with statistical mechanical calculations. The kinetics of the reaction is also discussed.

Experimental

Preliminary Remarks. The gas phase reaction N₂O₄(g) \rightleftharpoons 2 NO₂(g) is a favorite textbook example for the

Table 1. Some Gaseous Nitrogen Oxides

Formula	Structure ^a	Name	Remarks	Relevance
N ₂ O		nitrous oxide	colorless radical	greenhouse gas; precursor of the stratospheric NO
NO		nitric oxide	colorless radical	neurotransmitter; depletes stratospheric ozone
NO ₂		nitrogen dioxide	yellow-brown radical	atmospheric pollutant; precursor of tropospheric ozone
N ₂ O ₄		dinitrogen tetroxide	colorless; with planar structure	rocket propellant; nonaqueous solvent
NO ₃		nitrogen trioxide	blue radical; very reactive	atmospheric pollutant

^aBond lengths in Å.

discussion of chemical equilibrium [5], and its experimental study is described in an article [6] and in several physical chemistry laboratory manuals [7–9]. Two methods have been used: pressure measurements in conjunction with weighing [7–9] and spectrophotometry [6]. The first method requires very accurate mass measurements, and, for this reason, large volumes are required along with a vacuum line. The spectrophotometric method, as described in the literature [6], also requires a vacuum line, and the experiment is performed at a single wavelength, the only purpose being the determination of the equilibrium constant. Present safety concerns and the trend towards the use of the smallest possible amounts render the implementation of the aforementioned experiments difficult if not impossible. In this work, a new method, simultaneously simpler and more precise, is described, which also allows the determination of the absorption spectra of the monomer and of the dimer. Unlike the published experimental techniques that use NO₂ gas cylinders, and require large volumes, in the present method the nitrogen oxides are prepared with good purity and in small amounts from common starting materials.

NO₂ Preparation. NO₂ (very poisonous gas! Lethal above 200 ppmv [10]) is obtained by the reaction of nitric acid with metallic copper in the form of thin foils in a well-ventilated fume hood [1]. Gloves should be used throughout the experiment in order to avoid damage to the skin by the vapors and by the acid. The formed NO immediately reacts with atmospheric oxygen to give NO₂ vapor [1]. Part of the vapor is collected using a syringe or a Pasteur pipette. The gas is next forced into a quartz absorption cell (1-cm path length) with a valve that is closed immediately after the injection. The concentration of nitrogen oxides inside the cell is adjusted in order to have a room-temperature absorbance of about 0.4 at 410 nm. The mixture contained in the cell is in this way made of nitrogen oxides (ca. 10⁻³ M) and air (ca. 4 × 10⁻² M), with a room temperature pressure of about 1 bar. In the absence of strong UV-vis radiation, the presence of O₂ and N₂ does not affect the equilibrium, but only the corresponding kinetics (effect to be discussed below). The above described preparation can be performed either by the students, under close supervision, or ahead of time by the instructor.

Recording the Absorption Spectra After recording the baseline with two empty cells, the absorption spectrum of the gaseous mixture is recorded (220 nm to 800 nm) as a function of temperature (e.g., from 5 °C to 75 °C, every 10 °C). It is important to check the reproducibility of the results by measuring the absorption spectra at each temperature twice, once as temperature is incrementally increased (e.g., from 5 °C to 75 °C) and again as temperature is incrementally decreased (e.g., from 75 °C to 5 °C). The spectra are stored as ASCII files for the subsequent numerical calculations using a spreadsheet (e.g., Microsoft Excel). As the pressure inside the cell increases with temperature, care must be exercised, and the temperature should not exceed the maximum preset value. In the absence of vaporizable liquids, like water (to be totally avoided), the

pressure increases by less than 20% when going from room temperature to 75 °C. In the present work, spectra were recorded in a UV-Vis-NIR Shimadzu 3101PC spectrophotometer equipped with a temperature controller. The spectra were recorded with 0.2-nm slits, and data was stored every 0.5 nm.

Results and Discussion

Monomer–Dimer Equilibrium. For the equilibrium N₂O₄(g) ⇌ 2 NO₂(g), there is an equilibrium constant, K_p ,

$$K_p = \frac{(p_M/p_0)^2}{p_D/p_0} \quad (6)$$

where M is the monomer (NO₂), D is the dimer (N₂O₄), and p_0 is the standard-state pressure (1 bar). Owing to the low pressures involved, deviations from ideality are negligible.

The mole fraction x of monomeric NO₂ is,

$$x = \frac{[M]}{[M]_\infty} \quad (7)$$

where $[M]_\infty$ is the total (analytical) concentration of NO₂,

$$[M]_\infty = [M] + 2[D] \quad (8)$$

It can be obtained from eqs 6 through 8 that

$$x = \frac{2}{1 + \sqrt{1 + \frac{8[M]_\infty}{K_p c_0}}} = \frac{2}{1 + \sqrt{1 + \frac{8[M]_\infty}{K_c}}} \quad (9)$$

where c_0 is the standard concentration, corresponding to the pressure of 1 bar ($c_0 = p_0/RT$), being, therefore, a temperature-dependent quantity, and K_c is the concentration equilibrium constant. Given that the reaction is endothermic, the equilibrium shifts towards the monomer as the temperature is increased. This result is valid for both constant pressure and constant volume.



Figure 1. Visual appearance of a $\text{NO}_2 + \text{N}_2\text{O}_4$ mixture at 15 °C (left) and at 75 °C (right).

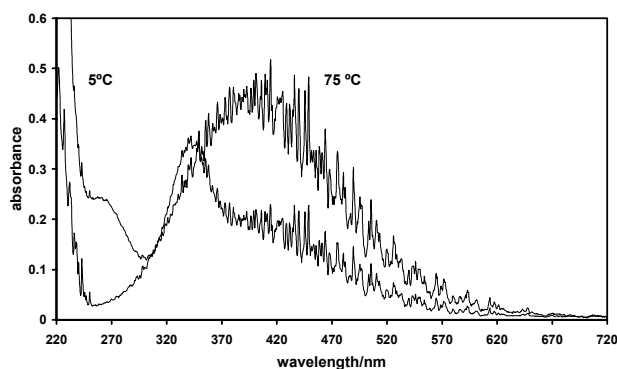


Figure 2. Absorption spectra of the mixture $\text{NO}_2 + \text{N}_2\text{O}_4$, at 5 °C and at 75 °C.

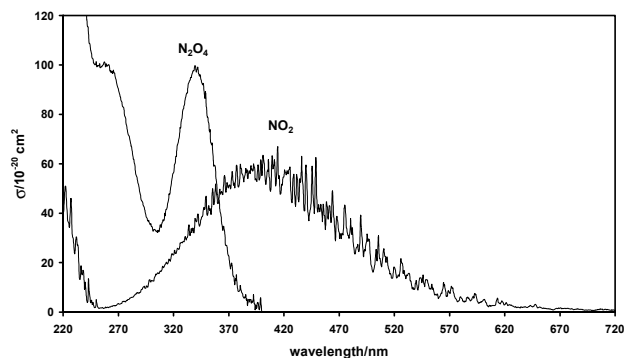


Figure 3. Computed absorption spectra of pure NO_2 and pure N_2O_4 .

Absorption: Qualitative Aspects. The direct observation of the color of the cell as a function of temperature shows the shift of the equilibrium. At room temperature, the gas is pale, but heating the cell for a few moments with a hair dryer, for instance, noticeably intensifies its color, see Figure 1. The absorption spectrum of the mixture is shown in Figure 2 for the lowest and highest temperatures of the study: 5 °C and 75 °C, respectively. It is thus seen that the color intensification results from an increased absorption in the visible (>380 nm). It is also observed that the two spectra coincide for two narrow

wavelength ranges: 310 to 312 nm and 349 to 351 nm. At these so-called isosbestic points, monomer and dimer absorption coefficients obey the relation [11]

$$\varepsilon_{\text{M}}(\lambda_{\text{iso}}) = \varepsilon_{\text{D}}(\lambda_{\text{iso}})/2 \quad (10)$$

The complex fine structure of the spectra is not due to noise, resulting instead from many vibronic transitions in the absorption spectrum of NO_2 (see Figure 3) [12–14]. In contrast, the dimer spectrum is smooth with insignificant fine structure (see Figure 3) [12–14].

Absorption Spectra: Method of Analysis. For a given temperature, the absorbance of the mixture is

$$A(\lambda) = a_{\text{M}}(\lambda)[\text{M}] + a_{\text{D}}(\lambda)[\text{D}] \quad (11)$$

where

$$\begin{aligned} a_{\text{M}}(\lambda) &= \varepsilon_{\text{M}}(\lambda)l \\ a_{\text{D}}(\lambda) &= \varepsilon_{\text{D}}(\lambda)l \end{aligned} \quad (12)$$

and where l is the optical path and ε_{M} and ε_{D} are the monomer and dimer molar absorption coefficients, respectively. From

$$\begin{aligned} [\text{M}] &= x[\text{M}]_{\infty} \\ [\text{D}] &= \frac{1-x}{2}[\text{M}]_{\infty} \end{aligned} \quad (13)$$

it is obtained that

$$A(\lambda) = \left[a_{\text{M}}(\lambda) - \frac{a_{\text{D}}(\lambda)}{2} \right] [\text{M}]_{\infty} x + \frac{a_{\text{D}}(\lambda)}{2} [\text{M}]_{\infty} \quad (14)$$

which can be rewritten as

$$A(\lambda) = \left[A_{\text{M}}^0(\lambda) - \frac{A_{\text{D}}^0(\lambda)}{2} \right] x + \frac{A_{\text{D}}^0(\lambda)}{2} \quad (15)$$

where $A_{\text{M}}^0(\lambda)$ and $A_{\text{D}}^0(\lambda)$ are the pure monomer and dimer absorbances for a concentration equal to $[\text{M}]_{\infty}$. Above 400 nm, the dimer absorption is negligible [12–15], and eq 15 reduces to

$$A(\lambda) = A_{\text{M}}^0(\lambda)x \quad (16)$$

From the measurement of the spectrum at two temperatures, T_1 and T_2 ($T_2 > T_1$), and assuming that the spectra of both monomer and dimer are essentially temperature independent (this assumption is supported by the existence of isosbestic points), the following ratio is defined

$$\beta = \frac{x_1}{x_2} = \frac{A_1(\lambda)}{A_2(\lambda)} \quad (17)$$

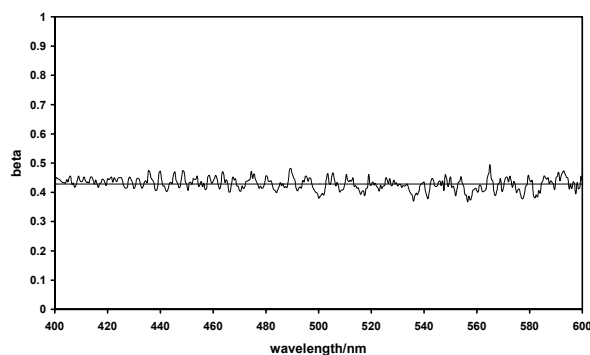


Figure 4. β parameter (eq 17). The average value is $\beta = 0.429 \pm 0.002$.

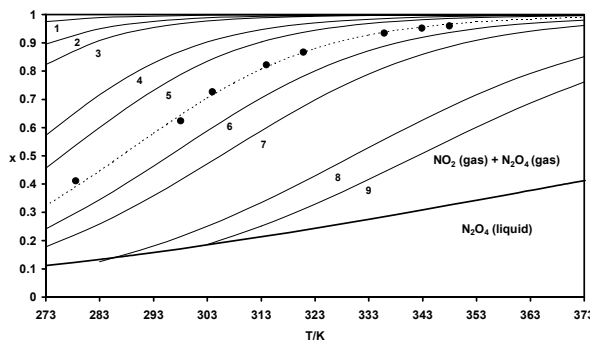


Figure 5. Molar fraction of NO_2 present as a monomer as a function of temperature and analytic concentration. Experimental results (\bullet) and curves are computed according to eq 9. $[\text{M}]_\infty = 10^{-5}$ M (1), 5×10^{-5} M (2), 10^{-4} M (3), 5×10^{-4} M (4), 10^{-3} M (5), 5×10^{-3} M (6), 10^{-2} M (7), 5×10^{-2} M (8), 0.1 M (9). The liquid–vapor equilibrium line is also shown. Below this line, only liquid exists. The dimer is largely predominant (>99.9%) in the liquid.

From this ratio ($\lambda > 400$ nm) the calculation of $A_D^0(\lambda)$ follows, given that

$$\beta A_2(\lambda) - A_1(\lambda) = \frac{A_D^0(\lambda)}{2}(\beta - 1) \quad (18)$$

hence,

$$A_D^0(\lambda) = \frac{2}{\beta - 1} [\beta A_2(\lambda) - A_1(\lambda)] \quad (19)$$

It is, therefore, possible to obtain the dimer spectrum from two spectra of the mixture measured at different temperatures but at constant analytical concentration.

In order to compute the monomer absorption spectrum, eq 15 is used again,

$$A_M^0(\lambda) = \frac{1}{x} \left[A(\lambda) - \frac{1-x}{2} A_D^0(\lambda) \right] \quad (20)$$

Nevertheless, the spectrum is now a function of the monomer mole fraction, x , which is not known. For a sufficiently high temperature, $x = 1$ and the recorded spectrum is the spectrum of the pure monomer. On the other hand, if the spectrum of the

monomer is taken from a spectral library, matching $A_M^0(\lambda)$ with the published spectrum allows the simultaneous determination of $[\text{M}]_\infty$ and of x . This is performed by a nonlinear least-squares fitting to the published spectrum using eq 20. Equation 15 can then be used to compute the monomer molar fraction at all temperatures,

$$x = \frac{A(\lambda) - \frac{A_D^0(\lambda)}{2}}{A_M^0(\lambda) - \frac{A_D^0(\lambda)}{2}} \quad (21)$$

This was the procedure followed in this work because a significant amount of dimer still existed at the highest attained temperature.

Absorption Spectra: Results. The method of data analysis described above was applied to the spectra obtained at 5 °C and at 75 °C. The parameter β (eq 17) was computed for wavelengths between 400 nm and 600 nm (Figure 4). As can be seen in Figure 4, this parameter is constant within experimental error, thus confirming that the dimer does not absorb significantly above 400 nm. The average value, computed with 400 points, is $\beta = 0.429 \pm 0.002$.

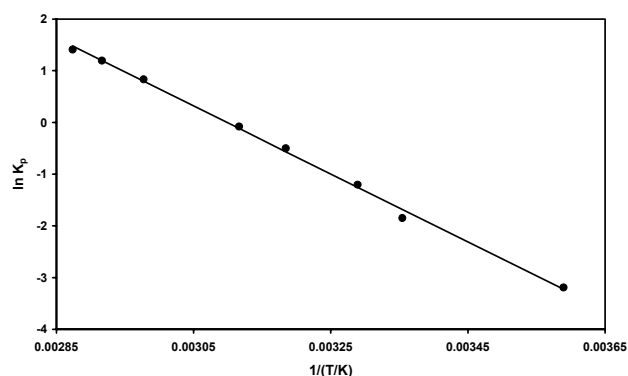
The spectrum of the pure dimer with concentration $[\text{M}]_\infty$, $A_D^0(\lambda)$, was next obtained from eq 19. Using eq 15 at this point, with trial values of x , shows that the monomer mole fraction at 75 °C must be higher than 0.94, otherwise negative absorbances are obtained for wavelengths around 260 nm. The precise value of x is obtained by matching the computed $A_M^0(\lambda)$, which is a function of x , with the published spectrum available in digital format [16]. An excellent agreement is obtained for $x = 0.96$. The value of the parameter $[\text{M}]_\infty$ (analytical concentration) corresponding to this mole fraction was $[\text{M}]_\infty = 3.1 \times 10^{-3}$ M. Dividing $A_D^0(\lambda)$ by this value, the dimer absorption coefficients are finally obtained. Once again, comparison of the calculated dimer absorption with the published dimer spectrum in digital format shows a very good agreement; however, the computed spectrum displays less noise and no discontinuities. The computed monomer and dimer spectra are shown in Figure 3. Note that the values of the absorption coefficients of the monomer can be a function of the spectrophotometer slits used, given the fine structure of the spectrum.

It should be mentioned that the obvious method for obtaining the monomer absorption spectrum is dilution. In a sufficiently dilute sample, almost all of the NO_2 is present in the monomer form; however, at room temperature and for a 1-cm-pathlength cell the required dilution is too high (see Figure 5). With very dilute samples, the spectrum is usually noisy and can be distorted by impurities.

Thermodynamic and Statistical Mechanical Calculations. After the calculation of $A_M^0(\lambda)$ and $A_D^0(\lambda)$ from the spectra, the mole fraction of monomeric NO_2 , x , is calculated for each temperature using eq 21. The wavelength range where the spectral differences are more pronounced, 220 to 280 nm, yields values of x that are almost wavelength-independent. The average x values computed (from 120 points for each temperature), which are quite precise, are displayed in Figure 5.

Table 2. Temperature Dependence of the Measured Molar Fraction of Monomeric NO₂ and of the Equilibrium Constant

T/°C	5.4	24.9	30.8	40.8	47.7	62.7	69.7	74.8
<i>x</i>	0.41	0.62	0.73	0.82	0.87	0.94	0.95	0.96
<i>K_p</i>	0.041	0.16	0.30	0.61	0.92	2.3	3.3	4.1

**Figure 6.** van't Hoff plot for the reaction N₂O₄(g) ⇌ 2 NO₂(g).**Table 3.** Spectroscopic Entropies of NO₂ and of N₂O₄ and Entropy of the Reaction N₂O₄(g) ⇌ 2 NO₂(g) (298 K, 1 bar)

Entropy/J K ⁻¹ mol ⁻¹	N ₂ O ₄	NO ₂	Δ _r S ⁰
translational	165.2	156.6	148.0
rotational	97.9	76.5	55.2
vibrational	41.6	1.2	-39.3
electronic	0	5.8	11.5
total	304.7	240.1	175.4
published value	304.4	240.0	175.6

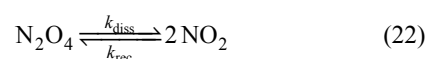
With these mole fractions, the equilibrium constants *K_p* are obtained from eq 9 solved for *K_p*. The results are given in Table 2.

The plot of ln *K_p* versus 1/*T* (van't Hoff plot), Figure 6, is linear. The reaction enthalpy, Δ_r*H*⁰, is obtained from the slope, while the reaction entropy, Δ_r*S*⁰, is obtained from the intercept. The linearity of the plot shows that these values are constant in the experimental temperature range.

The values obtained were Δ_r*H*⁰ = 55 ± 3 kJ mol⁻¹ and Δ_r*S*⁰ = 169 ± 8 J K⁻¹ mol⁻¹, in good agreement with the published values for 298 K [1, 17], Δ_r*S*⁰ = 57.2 kJ mol⁻¹ and Δ_r*S*⁰ = 176 J K⁻¹ mol⁻¹. The measured reaction enthalpy is, in fact, the dissociation enthalpy of the dimer N–N bond, *DH*⁰(N–N). Its value is remarkably small. This result is compatible with the exceptionally long length of the N–N bond in the dimer, 1.77 Å [18]. For comparison, in hydrazine, which also has a single N–N bond, the bond length is 1.45 Å, whereas the respective enthalpy is 275 kJ mol⁻¹ [19]. The molar entropies of NO₂ and N₂O₄, and therefore also the reaction entropy, can be obtained from statistical mechanical calculations [20]. Using the structural and spectroscopic data available in the literature (angles and bond lengths [1, 18], vibration frequencies [21, 22]), and using the perfect gas model (translational entropy), the classical rigid rotor model (rotational entropy), and the harmonic oscillator model (vibrational entropy [23]), the respective contributions to the total entropy were computed as shown in Table 3. The agreement with the published values for the entropies of NO₂, of N₂O₄, and of the reaction [1, 17] is very satisfactory.

From the known dependence of *K_p* on *T* and using eq 9, it is possible to compute the fraction of monomer, *x*, as a function of *T* and of [M]_∞ as shown in Figure 5. This diagram allows a quick evaluation of the temperature and analytical concentration conditions under which the monomer or the dimer are the dominant species. It is also seen that for very high analytical concentrations condensation can occur, the normal boiling point of dinitrogen tetroxide being 21 °C [1].

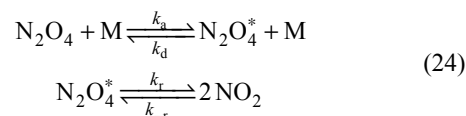
Kinetics of the Reaction. The study of the dimerization equilibrium leads very naturally to the desire to know the kinetics of the reaction. Unfortunately, the kinetics is too fast. The equilibrium is attained in a few milliseconds, or even less, and the kinetics cannot be studied with the kind of equipment usually available in the undergraduate laboratory. Notwithstanding, it is appropriate to discuss the kinetics of the reaction, precisely to understand why it is so fast. The reaction can be written as



with

$$K_c = \frac{k_{\text{diss}}}{k_{\text{rec}}} \quad (23)$$

The direct reaction is a unimolecular gas-phase process; therefore, it can be written as a Lindemann mechanism (in a semiquantitative description),



where N₂O₄* is the energized molecule and M is a third body (mainly, N₂ or O₂ for the reaction in air).

Application of the steady-state approximation to N₂O₄* leads to

$$\begin{aligned} k_{\text{diss}} &= \frac{k_{\text{a}} k_{\text{r}} [\text{M}]}{k_{\text{r}} + k_{\text{d}} [\text{M}]} \\ k_{\text{rec}} &= \frac{k_{\text{d}} k_{-r} [\text{M}]}{k_{\text{r}} + k_{\text{d}} [\text{M}]} \end{aligned} \quad (25)$$

The rate constants of the forward and backward reactions are, therefore, a function of total pressure; however, *K_p* and *K_c* are pressure independent. In the high-pressure limit ([M] → ∞, in practice tens of bar)

$$\begin{aligned} k_{\text{diss}}^{\infty} &= \frac{k_{\text{a}} k_{\text{r}}}{k_{\text{d}}} \\ k_{\text{rec}}^{\infty} &= k_{-r} \end{aligned} \quad (26)$$

These rate constants have been evaluated experimentally (255 to 273 K) [24], and are given by

$$k_{\text{diss}}^{\infty} / \text{s}^{-1} = 2.8 \times 10^{13} T^{1.3} \exp\left(-\frac{6790}{T}\right) \quad (27)$$

$$k_{\text{rec}}^{\infty} / \text{M}^{-1} \text{s}^{-1} = 2.2 \times 10^3 T^{2.3}$$

In this way, the rate constants at 298 K take the following estimated values:

$$k_{\text{diss}}^{\infty} = 5.9 \times 10^6 \text{ s}^{-1} \quad (28)$$

$$k_{\text{rec}}^{\infty} = 1.1 \times 10^9 \text{ M}^{-1} \text{ s}^{-1}$$

in good agreement with values directly measured at this temperature [25]. The pre-exponential factor of the dissociation rate constant is, at 298 K, $4.6 \times 10^{16} \text{ s}^{-1}$. This value is indicative of a loose transition state, that is, a transition state where the bond-breaking process is well advanced. The activation energy of the dissociation reaction (56.5 kJ mol^{-1}) coincides with the dimer bond dissociation energy given that the reverse reaction, radical recombination, is essentially nonactivated.

Knowledge of the rate constants (in the high-pressure limit) allows the estimation of the relaxation time of the reaction. For the mechanism corresponding to eq 22, the relaxation time is given by

$$\tau = \frac{1}{k_{\text{diss}} + 4k_{\text{rec}}[\text{NO}_2]} = \frac{1}{k_{\text{rec}}} \frac{1}{K_c + 4[\text{NO}_2]} \quad (29)$$

hence, a relaxation time of 100 ns at 298 K is predicted for $[\text{NO}_2] = 10^{-3} \text{ M}$. For lower third-body concentrations, the relaxation time is never higher than a few ms, and it can be concluded that the equilibrium always responds very quickly to any perturbation.

An historical perspective of the kinetic studies of the $\text{N}_2\text{O}_4(\text{g}) \rightleftharpoons 2 \text{NO}_2(\text{g})$ reaction, covering a time span of 115 years, was recently published [26].

Conclusions

The approach described here allows the integration of thermodynamic, kinetic, and spectroscopic aspects for the reversible gas-phase reaction $\text{N}_2\text{O}_4(\text{g}) \rightleftharpoons 2 \text{NO}_2(\text{g})$. Only relatively common equipment and chemicals are required for the experiment. It consists of the (optional) synthesis of NO_2 and the study of the UV-vis electronic absorption spectrum of the $\text{NO}_2/\text{N}_2\text{O}_4$ gas mixture as a function of temperature. From the analysis of the spectra, the absorption spectra of the pure constituents are obtained as well as the temperature dependence of the equilibrium constant of the reaction. From this dependence, the enthalpy and the entropy of the reaction were obtained. The values were analyzed and compared with statistical mechanical calculations. The kinetics of the reaction was also discussed.

Other aspects that can be included in a project on this reaction are studies of the chemical bonding in both monomer and dimer, of the electronic structure and electronic transitions observed, and of the monomer and dimer photodissociation reactions.

Acknowledgment. We thank Prof. Manuel E. Minas da Piedade (FCUL, Lisbon) and Prof. José A. Martinho Simões (FCUL, Lisbon) for helpful discussions.

References and Notes

- (a) Jones, K. *The Chemistry of Nitrogen*; Pergamon Press: Oxford, 1975; (b) Greenwood, N. N.; Earnshaw, A. *Chemistry of the Elements*, 2nd ed.; Butterworth-Heinemann: Oxford, 1997.
- Dulong was a French physical chemist (1785–1838), best known from the Dulong and Petit rule. In 1812 he discovered NCl_3 , highly explosive, in whose study he lost one eye and two fingers of his right hand. He also studied nitrogen oxides and water vapor at high pressures. Dulong died at a relatively young age, leaving his family in a difficult economic situation because most of his income had been used to buy material and laboratory equipment and not set aside as savings. The accuracy of some of the experimental results used by Dulong and Petit for the establishment of their law have been questioned recently, see Giunta, C. J. *Bull. Hist. Chem.* **2002**, *27*, 62–71.
- Finlayson-Pitts, B. J.; Pitts Jr., J. N. *Chemistry of the Upper and Lower Atmosphere*; Academic Press: New York, 2000.
- Turns, S. R. *An Introduction to Combustion*; McGraw-Hill: New York, 1996.
- Yang, Z. *J. Chem. Educ.* **1993**, *70*, 94–95.
- Wettack, F. S. *J. Chem. Educ.* **1972**, *49*, 556–558.
- Daniels, F.; Williams, J. W.; Bender, P.; Alberty, R. A.; Cornwell, C. D.; Harriman, J. E. *Experimental Physical Chemistry*, 7th ed.; McGraw-Hill: New York, 1970.
- Sime, R. J. *Physical Chemistry—Methods, Techniques, and Experiments*; Saunders: Philadelphia, 1990.
- Halpern, A. M. *Experimental Physical Chemistry*, 2nd ed.; Prentice-Hall: Upper Saddle River, NJ, 1997.
- The olfactory threshold, 0.1 ppmv, is fortunately much lower. Considering the equation $8 \text{HNO}_3 + \text{O}_2 + 3 \text{Cu} \rightarrow 2 \text{NO}_2 + 3 \text{Cu}(\text{NO}_3)_2 + 4 \text{H}_2\text{O}$ and assuming that both acid and oxygen are in excess, the amount of NO_2 produced is controlled by the initial mass of copper. In order to attain a 100-ppmv ($4 \times 10^{-6} \text{ M}$) level of NO_2 in a small room ($5 \times 5 \times 3 \text{ m}^3$), 19 g (0.3 mol) of copper are required. The danger of NO_2 is due to its reaction with the water present in the respiratory tract, producing nitric and nitrous acids, and also owing to the oxidation of biological compounds with the production of the nitrite ion (NO_2^-). The mass of copper used in this work was approximately 2 g.
- In atmospheric chemistry, it is common practice to work with the molar absorption coefficient, σ , defined by the Beer-Lambert law written as $I = I_0 e^{-\sigma N l}$, where I_0 is the intensity of the incident beam, I is the transmitted intensity, σ is the molar absorption coefficient (in $\text{cm}^2 \text{ molecule}^{-1}$), N is the number of molecules per cm^3 , and l is the path length (in cm). It follows that $\sigma (\text{M}^{-1} \text{ cm}^{-1}) = 2.62 \times 10^{20} (\sigma \text{ cm}^2)$.
- Hall, T. C.; Blacet, F. E. *J. Chem. Phys.* **1952**, *20*, 1745–1749.
- Schneider, W.; Moortgart, G. K.; Tyndall, G. S.; Burrows, J. P. *J. Photochem. Photobiol. A* **1987**, *40*, 195–217.
- Harwood, M. H.; Jones, R. L. *J. Geophys. Res.* **1994**, *99*, 22955–22964.
- This assumption is justified *a posteriori* by the independence of β with respect to the wavelength (cf. Figure 4).
- Nölle, A.; Pätzold, F.; Pätzold, S.; Meller, R.; Moortgart, G. K.; Röth, E. P.; Ruhnke, R.; Keller-Rudek, H. *UV/Vis Spectra of Atmospheric Constituents*; ATMOS, DFD, 1998.
- Roscoe, H. K.; Hind, A. K. *J. Atmos. Chem.* **1993**, *16*, 257–276.
- Shen, Q.; Hedberg, K. *J. Phys. Chem. A* **1998**, *102*, 6470–6476.
- Lide D. R., Ed., *CRC Handbook of Chemistry and Physics*, 79th ed.; CRC Press: Boca Raton, 1998.

20. McClelland, B. J. *Statistical Thermodynamics*; Chapman and Hall: London, 1982.
21. Mélen, F.; Pokorni, F.; Herman, M. *Chem. Phys. Lett.* **1992**, *194*, 181–186.
22. Koput, J.; Seibert, J. W. G.; Winnewisser, B. P. *Chem. Phys. Lett.* **1993**, *204*, 183–189.
23. For the lowest frequency normal vibration mode of N₂O₄ (ca. 60–80 cm⁻¹), which is a torsional mode, the partially hindered linear-rotor model was used.
24. Markwalder, B.; Gozel, P.; Bergh, H. *J. Chem. Phys.* **1992**, *97*, 5472–5479.
25. Borrell, P.; Cobos, C. J.; Luther, K. *J. Phys. Chem.* **1988**, *92*, 4377–4384.
26. Bauer, S. H. *Chem. Rev.* **2002**, *102*, 3893–3903.